

## Multiple Excitation at Xenon 5s Photoionization Threshold

J. Tulkki

Research Institute for Theoretical Physics, University of Helsinki, 00170 Helsinki, Finland  
and Laboratory of Physics, Helsinki University of Technology,<sup>(a)</sup> 02150 Espoo, Finland

(Received 28 March 1989)

The effect of multiple-electron excitation on the threshold behavior of Xe 5s photoionization is studied using the multichannel multiconfiguration Dirac-Fock method with full account of relaxation. The inclusion of the ionization channels related to  $5p^4 5d J_{\text{ion}} = \frac{1}{2}$  excited states is found to change the single-excitation results drastically. Our cross section and asymmetry parameter  $\beta$  are in very good agreement with experiment. Calculation of the related satellite cross sections predicts a new type of satellite that exists only in the near-threshold region and has a peculiar angular dependence.

PACS numbers: 32.80.Fb

The photoelectron spectrum is a unique and selective probe of two-electron excitations in free atoms. Thus the experimental Ne 2s and Ar 3s photoelectron satellite spectra have a rich structure, which depends strongly on the photon energy in the near-threshold region.<sup>1-4</sup> The Xe 5s satellite spectrum has also been measured in the vicinity of the Cooper minimum of the 5s main line but with lower resolution.<sup>5</sup> Hence the energy dependence of the individual satellite lines is less clear in this case. In spite of a multitude of experimental data,<sup>1-5</sup> there has not been comparable progress on the theoretical side. For Xe 5s photoionization it has been suggested that the coupling between the 5s hole and the  $5p^{-2} 5d J_{\text{ion}} = \frac{1}{2}$  states would significantly affect the intensity and angular dependence of the 5s main line.<sup>6</sup> This mixing, which also includes the interaction between single- and double-hole ionization channels, would obviously be equally important for the near-threshold behavior of the related satellite lines. Double excitations are evidently not included in the most extensive relativistic random-phase-approximation (RRPA) calculation of the Xe 5s partial cross section and  $\beta$  parameter.<sup>7</sup> This may explain why the RRPA calculation is in striking contradiction with experiments.<sup>8</sup> In contrast, the relativistic time-dependent local-density approximation (RTDLDA), which includes correlation by a model potential, shows better agreement especially for the  $\beta$  parameter.<sup>9</sup> At higher photon energies the RTDLDA 5s partial cross section is, however, at variance with experiments by almost an order of magnitude.

In this Letter we report the first *ab initio* calculation of a photoionization process where the single- and double-hole ionization channels are treated exactly on the same footing. The interaction between the double-excitation channels and the most important single-excitation channels has been treated using the multichannel multiconfiguration Dirac-Fock (MMCDF) method. The relaxation was fully included by not only using separately optimized initial and final bound-state orbitals but by also including all overlap integrals in the photon-electron interaction matrix elements.<sup>10</sup> For the

final ionic core state we used orbitals optimized with respect to the 5s-hole configuration. The discrete and continuum orbitals representing excited electrons were calculated in the field of the 5s-hole configuration keeping the previously optimized orbitals frozen. The Lagrangian multipliers were used to enforce orthogonality between the excited and core orbitals.<sup>10</sup> The calculation of the final-state many-electron wave function was carried out in two steps. To account for the correlation in the final state of the ion, a configuration-integration (CI) calculation including 5s-hole configuration and the  $5p^{-2} 5d J_{\text{ion}} = \frac{1}{2}$  configurations was first carried out. In *jj* coupling this gives the following six configurations:

$$\begin{aligned}
 \Psi_1 &= |5s^{-1}; J_{\text{ion}} = \frac{1}{2}\rangle, \\
 \Psi_2 &= |5p_{1/2}^{-1}, 5p_{3/2}^{-1} (J=1), 5d_{1/2}; J_{\text{ion}} = \frac{1}{2}\rangle, \\
 \Psi_3 &= |5p_{1/2}^{-1}, 5p_{3/2}^{-1} (J=2), 5d_{3/2}; J_{\text{ion}} = \frac{1}{2}\rangle, \\
 \Psi_4 &= |5p_{1/2}^{-1}, 5p_{3/2}^{-1} (J=2), 5d_{1/2}; J_{\text{ion}} = \frac{1}{2}\rangle, \\
 \Psi_5 &= |5p_{3/2}^{-2} (J=2), 5d_{3/2}; J_{\text{ion}} = \frac{1}{2}\rangle, \\
 \Psi_6 &= |5p_{3/2}^{-2} (J=2), 5d_{1/2}; J_{\text{ion}} = \frac{1}{2}\rangle.
 \end{aligned} \tag{1}$$

The energies of the eigenvectors obtained by diagonalizing the ionic Hamiltonian are given in Table I together with experimental data from Ref. 5, and values obtained from a separate extensive CI calculation are discussed in detail below.

At the second step the initial- and final-state orbitals and the ionic eigenvectors generated using the MCDF code of Grant *et al.*<sup>11</sup> were used as input data for our relativistic *K*-matrix code.<sup>12</sup> The photoelectron continuum wave functions  $\epsilon l j$  ( $l=1; j=\frac{1}{2}, \frac{3}{2}$ ) were coupled to the ionic eigenvectors resulting in 12 ionization channels. In analogy to earlier RRPA calculations<sup>7</sup> we also included singly excited channels pertaining to final 5p and 4d hole states. This gives altogether 23 channels. For reference purposes we also carried out calculations which included only single-excitation channels corresponding to final 5s, 5p, and 4d hole states (13 channels) and only 5s

TABLE I. Calculated and experimental binding energies (eV) and line assignments. The satellite energies are given with respect to the main line. The notation ( $^1D$ ) refers to the  $5s^25p^4$  configuration.

	Calc. 1 <sup>a</sup>	Calc. 2 <sup>b</sup>	Expt. <sup>c</sup>	Final state <sup>d</sup>
Main line	24.83	23.81	23.40	$5s5p^6\ ^2S_{1/2}$
Satellite				
1	0.51	0.68		
2	1.11	1.47		
3	1.65	1.80		
4 (7)	3.39	3.94	4.18	
5 (9)	4.31	5.42	5.5	( $^1D$ ) $5d\ ^2S_{1/2}$

<sup>a</sup>CI calculation including 6 configurations, given in Eq. (1).

<sup>b</sup>CI calculation including 34 configurations as described in text.

<sup>c</sup>Experimental data from Ref. 5. The satellite indices in parentheses correspond to numbering of peaks in Ref. 5.

<sup>d</sup>The  $LS$  assignment does not correspond to the real physical situation as pointed out in text.

and  $5p$  hole states (7 channels).

In the calculation of the transition amplitudes single-configuration ground-state orbitals were used for the initial state. The incomplete orthogonality of the initial- and final-state orbitals was fully taken into account as explained above.<sup>10</sup> The transition amplitudes were calculated in the velocity gauge using the dipole approximation. Unlike RPA, MMCDF does not necessarily give gauge-invariant transition amplitudes when a limited number of configurations and channels are included to account for the correlation effects. However, our MMCDF cross sections and  $\beta$  parameters agree in the 7- and 13-channel cases within a few percent with the corresponding gauge-invariant RPA calculation.<sup>7</sup> For the threshold energies we used theoretical values corresponding to the 6-configuration CI calculation. For the  $5p$  and  $4d$  ionization energies single-configuration total energy differences with separately optimized initial and final states were used. It was found that the discrepancy of 1.43 eV between the experimental and theoretical  $5s$  threshold energies had only a small effect on the results except for an overall shift with respect to the photon energy scale. For the satellites the energy discrepancy is somewhat larger due to the limited 6-configuration CI function space.

The calculated photoelectron asymmetry parameter  $\beta$  and cross section of the  $5s$  photoionization are given in Figs. 1(a) and 1(b), respectively, as a function of the photon energy together with experimental data.<sup>13-18</sup> The theoretical curves start about 4.31 eV above the  $5s$  threshold since below this energy there are *autoionizing* states which cannot be treated consistently with the present version of the MMCDF code. In the 7- and 13-channel cases the curves are very similar to those obtained earlier by RPA.<sup>7</sup> The dotted line represents the

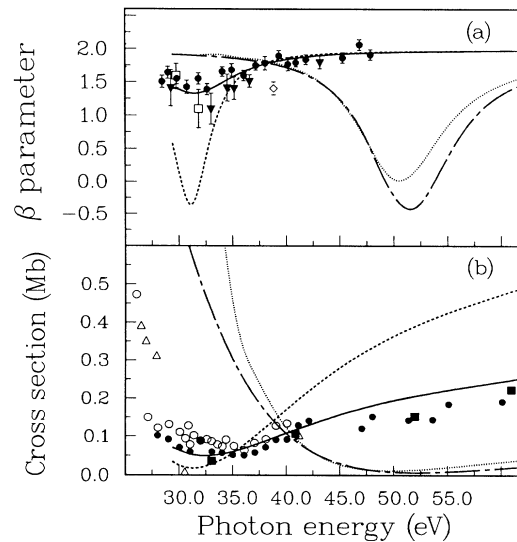


FIG. 1. Theoretical and experimental cross section and photoelectron asymmetry parameter for Xe  $5s$  photoionization. Theoretical curves: Solid line, 23-channel calculation; dashed line, 13-channel calculation; long-short-dashed line, 7-channel calculation; and dotted line, 7-channel calculation excluding relaxation. Experimental data: Solid dots, Ref. 8; open circles, Ref. 13; solid squares, Ref. 14; open squares, Ref. 15; solid inverted triangles, Ref. 16; open triangles, Ref. 17; diamond, Ref. 18.

result of a 7-channel calculation, which is otherwise identical to that described above, except that ground-state core orbitals have been used in the calculation of the final-state many-electron wave function. The comparison of the results shows that the effect of relaxation is not very significant. Inclusion of double-excitation channels results in a dramatic difference. Both the  $\beta$  parameter and the cross section are now in very good agreement with experiment. At large photon energies, where the sudden approximation<sup>19</sup> is applicable, the reduction of the  $5s$  cross section with respect to the 13-channel case is explained by the mixing of  $\Psi_1$  with double-hole states in Eq. (1). The effect of interchannel interaction becomes decisive at low photon energies where the cross section and especially the  $\beta$  parameter are increased, when the double-excitation channels are included.

The configuration space (1) is too small to give very accurate satellite energies or intensities.<sup>20</sup> In order to identify satellite peaks, extensive CI calculations were carried out to determine more accurate satellite energies. All  $jj$ -coupled configurations of the type  $5p^4nd\ J_{\text{ion}} = \frac{1}{2}$  with  $n=5, \dots, 9$  and  $5p^4ns\ J_{\text{ion}} = \frac{1}{2}$  with  $n=6, \dots, 9$  were included. In the first calculation the same orthogonal set of final-state orbitals as above was used. The results of this 34-configuration calculation are compared in Table I, together with values obtained from the 6-configuration calculation, with energies of selected satel-

lite peaks measured by Fahlman *et al.*<sup>5</sup> This comparison and a detailed analysis of the symmetry and component structure of the eigenvectors support our identification of experimental peak 9 as satellite 5. The same 34-configuration CI calculation was repeated using  $nd, ns$  orbitals calculated in the field of the  $5p^2$  double-hole core. The comparison between these two CI calculations shows that the first set of orbitals gives better estimates for the lowest satellite energies.

For comparison we also computed the Ar  $3s$  satellite energies by including 34 configurations of the type  $3p^4nd$   $J_{\text{ion}} = \frac{1}{2}$  with  $n=3, \dots, 7$  and  $3p^4ns$   $J_{\text{ion}} = \frac{1}{2}$  with  $n=4, \dots, 7$ . One-electron orbitals were calculated in the field of  $3s$  single-hole and  $3p^2$  double-hole core states. With the latter orbitals our results agree very well with previous calculations.<sup>20</sup> In contrast, the  $nd$  orbitals calculated in the field of the  $3s$ -hole configuration were excessively diffuse and consequently the satellite energies much too small. The difference between Xe  $5s$  and Ar  $3s$  ionization is mainly due to the partial collapse of the  $nd$  orbitals of Xe in comparison with Ar. Hence our 6-configuration CI calculation with  $5d$  orbitals solved in the field of the  $5s$ -hole state gives a rather good lowest-order description of the final-state correlation of the ion core.

The  $\beta$  parameters and cross sections of the three most intense satellite peaks, labeled 2, 4, and 5 in Table I, are given in Figs. 2(a) and 2(b), respectively, and are compared with experimental data by Fahlman *et al.*<sup>5</sup> The general behavior of the cross section and  $\beta$  parameter of satellite 5 (identified as the experimental peak 9) is very similar to that of the main line. However, the minima in the cross section and  $\beta$  parameter are shifted towards higher photon energies. A similar trend has been predicted for the  $3p^43d(^2S)$  satellite cross section in Ar using many-body perturbation theory.<sup>21</sup> The calculated  $\beta$  parameter of satellite 5 agrees very well with experiment, whereas the cross section clearly exceeds the experimental values<sup>5</sup> (not shown). This is a consequence of only including  $5p^45d$  satellite configurations in the multichannel calculation. Hence the cross sections in Fig. 2(b) effectively approximates the total  $5p^4nd$   $J_{\text{ion}} = \frac{1}{2}$ ,  $n=5, 6, \dots$ , satellite yield. If it is assumed that the coupling between these states and the  $5s$ -hole state is qualitatively similar for all  $n$  values, these satellites have nearly equal angular dependence explaining the good agreement between the theoretical and experimental  $\beta$  parameters in Fig. 2(a).

In contrast to Ar there is another  $5p^45d$   $J_{\text{ion}} = \frac{1}{2}$  satellite (satellite 2 in Table I) 1.4 eV above the main line, which has a high constant intensity well above the threshold. A comparison between the CI calculations for Ar and Xe show that the corresponding peak is not present in the Ar  $3s$  satellite spectrum. Hence it is a direct consequence of the spin-orbit interaction. For this satellite the minima are shifted towards lower photon en-

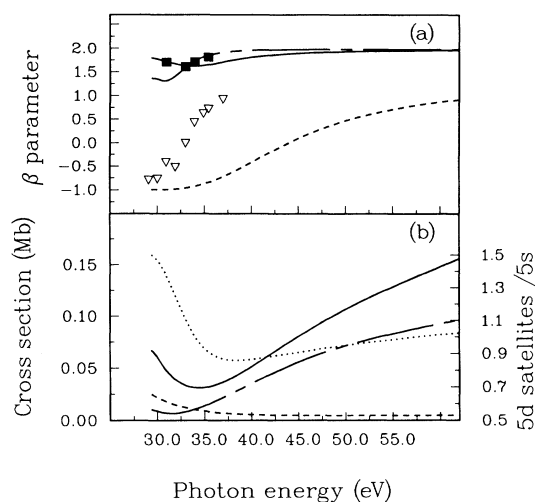


FIG. 2. Theoretical and experimental cross sections and asymmetry parameters for the most intensive  $5p^45d$  satellite processes. Theoretical curves: Solid line, satellite 5; dashed line, satellite 4; long-short-dashed line, satellite 2. Experimental data from Ref. 5: Solid squares, peak 9; open triangles, peak 7. The branching ratio of the calculated total  $5p^45d$  satellite intensity with respect to the intensity of the  $5s$  main line is given by the dotted line in (b).

ergies in comparison with the main line. It has so far not been identified in the low-resolution experimental spectrum.<sup>5</sup>

A peculiar new satellite is found in the threshold region. The ionic eigenvector corresponding to satellite 4 has only a very small  $5s$ -hole component and therefore it must disappear in the sudden-approximation region. The different physical origin of this satellite is reflected, as is shown in Fig. 2(a), by the photon energy dependence of its  $\beta$  parameter, in comparison with those of other satellites. The energy dependences of  $\beta$  of this satellite and the experimental peak 7<sup>5</sup> are surprisingly similar and they have nearly equal energies. Hence peak 7 has tentatively been identified with satellite 4 in Table I and Fig. 2(a). The detailed physical mechanism by which this satellite is produced requires further studies. Since it results from interchannel interactions it may be called an internal-electron-scattering (IES) satellite. The near-threshold  $3s$  satellites observed by Becker *et al.*<sup>1</sup> were also interpreted as IES satellites. However, they were associated with high-angular-momentum states of the final ion in contrast to the present satellite.

The ratio between the total intensity of satellites 1–5 and the intensity of the main line is also given in Fig. 2(b). The general behavior of the intensity ratio can be attributed to a shifted Cooper minimum in the leading satellite cross section. Unfortunately, no high-resolution measurements exist to make a comparison possible.

In conclusion, it has been shown by a relativistic *ab initio* calculation that the behavior of the Xe  $5s$  cross sec-

tion in the threshold region is largely determined by the interaction between the  $5s$  single-hole and  $5p^45d$  double-hole ionization channels. Our calculation also describes the behavior of the most prominent correlation satellites and shows that this interaction gives rise to a new IES photoelectron satellite line with special dynamical properties. The calculated satellite cross sections and asymmetry parameters are still approximative. More extensive calculations as well as new high-resolution measurements of the Xe  $5s$  satellite spectrum are consequently needed to reveal details of the dynamics of the near-threshold two-electron excitation.

The final calculation of the cross sections and  $\beta$  parameters took about 15 h of central-processing-unit time in an IBM 3090 180 VF (including a vector facility) computer. I want to thank the staff of the Computer Center of Helsinki University of Technology for help during various stages of this work. I am also grateful to Professor T. Åberg for inspiring discussions and critical reading of the manuscript. This work was supported by The Academy of Finland.

<sup>(a)</sup>Present address.

<sup>1</sup>U. Becker, B. Langer, H. G. Kerckhoff, M. Kupsch, D. Szostak, R. Wehlitz, P. A. Heimann, S. H. Liu, D. W. Lindle, T. A. Ferret, and D. A. Shirley, *Phys. Rev. Lett.* **60**, 1490 (1988).

<sup>2</sup>H. Kossman, B. Krässig, V. Schmidt, and J. E. Hansen, *Phys. Rev. Lett.* **58**, 1620 (1987).

<sup>3</sup>U. Becker, R. Hölzel, H. G. Kerckhoff, and B. Langer, *Phys. Rev. Lett.* **56**, 1120 (1986).

<sup>4</sup>K.-H. Schartner, B. Möbus, P. Lenz, H. Schmoranzner, and

M. Wildberger, *Phys. Rev. Lett.* **61**, 2744 (1988).

<sup>5</sup>A. Fahlman, M. O. Krause, T. A. Carlson, and A. Svensson, *Phys. Rev. A* **30**, 812 (1984).

<sup>6</sup>G. Wendin and A. F. Starace, *Phys. Rev. A* **28**, 3143 (1983).

<sup>7</sup>W. R. Johnson and K. T. Cheng, *Phys. Rev. Lett.* **40**, 1167 (1978); P. C. Deshmukh and S. T. Manson, *Phys. Rev. A* **32**, 3109 (1985).

<sup>8</sup>A. Fahlman, T. A. Carlson, and M. O. Krause, *Phys. Rev. Lett.* **50**, 1114 (1983).

<sup>9</sup>F. A. Parpia, W. R. Johnson, and V. Radojevic, *Phys. Rev. A* **29**, 3173 (1984).

<sup>10</sup>J. Tulkki and T. Åberg, *J. Phys. B* **18**, L489 (1985).

<sup>11</sup>I. P. Grant, B. J. McKenzie, P. H. Norrington, D. F. Mayers, and N. C. Pyper, *Comput. Phys. Commun.* **21**, 207 (1980).

<sup>12</sup>For the nonrelativistic  $K$ -matrix theory, see A. F. Starace, in *Handbuch der Physik XXXI*, edited by W. Mehlhorn (Springer-Verlag, Berlin, 1982).

<sup>13</sup>T. Gustafsson, *Chem. Phys. Lett.* **51**, 383 (1977).

<sup>14</sup>M.-Y. Adam, thesis, L'Universite de Paris-Sud, Centre d'Orsay, France, 1978 (unpublished).

<sup>15</sup>M. G. White, S. H. Southworth, P. Kobrin, E. D. Poliakoff, R. A. Rosenberg, and D. A. Shirley, *Phys. Rev. Lett.* **43**, 1661 (1979).

<sup>16</sup>H. Dehnenbach and V. Schmidt, *J. Phys. B* **16**, L337 (1983).

<sup>17</sup>J. A. R. Samson and J. L. Gardner, *Phys. Rev. Lett.* **33**, 671 (1974).

<sup>18</sup>J. L. Dehmer and D. Dill, *Phys. Rev. Lett.* **37**, 1049 (1976).

<sup>19</sup>T. Åberg, *Phys. Rev.* **156**, 35 (1967).

<sup>20</sup>H. Smid and J. E. Hansen, *J. Phys. B* **16**, 3339 (1983); A. Hibbert and J. E. Hansen, *J. Phys. B* **20**, L245 (1987), and references therein.

<sup>21</sup>W. Wijesundera and H. P. Kelly, *Phys. Rev. A* **36**, 4539 (1987).